Bearing capacity of strip footings subjected to complex loading

Luc Thorel, Abdul-Hamid Soubra, Josselin Garnier, Riad Assaf

Bearing capacity of strip footings subjected to complex loading

L. Thorel
Laboratoire Central des Ponts et Chaussées, Route de Bouaye, Bouguenais Cedex, France

A.-H. Soubra
GéM, Université de Nantes, Bd. de l'Université, Saint-Nazaire cedex, France

J. Garnier & R. Assaf
Laboratoire Central des Ponts et Chaussées, Route de Bouaye, Bouguenais Cedex, France

ABSTRACT: For shallow water systems installed on a sandy soil, the load applied to the footing may be complex (i.e. inclined and eccentric) and may include cyclic effects. This paper is limited to the study of the static behavior of a soil-footing system under inclined, eccentric or complex loading. Centrifuge tests on a small scale model of a strip footing placed on a horizontal sandy soil have been performed in the LCPC laboratory (Nantes) in France. Quasi-static force-controlled load, using hydraulic servo-jack, is applied to the footing. Experimental results of the bearing capacity are compared to those given by the kinematical approach of the limit analysis theory. Also, the experimental findings concerning the footing kinematics are presented and discussed. Finally, a comparison between the reduction coefficients obtained by centrifuge model tests and those given by the limit analysis theory is presented for different loading configurations.

1 INTRODUCTION

The calculation of the ultimate bearing capacity of shallow foundations is an old problem of soil mechanics. Numerous methods of computation of the ultimate bearing capacity are available in practice in the case of a central vertical load and a horizontal ground surface. These methods are based on either empirical techniques (e.g. Eurocodes 1996, DTU 1988, Fascicule62 1993, Vesic 1975) or simplified approaches (e.g. Caquot & Kérisel 1953). Some of them make use of laboratory shear strength characteristics of the soil (c', φ'), others refer to *in situ* test results (e.g. cone penetration or pressuremeter tests).

For a complex (inclined and eccentric) loading, the determination of the ultimate bearing capacity is more difficult. For instance, the methods based on in-situ tests are convenient only for a strip footing resting on a horizontal ground surface and subjected to a central vertical load. Also, the computation of the ultimate bearing capacity of a strip footing subjected to an inclined and/or eccentric load based on laboratory test results makes use of approximate empirical reduction coefficients to take into account the effect of load inclination and eccentricity. These empirical coefficients may significantly overestimate the true ultimate bearing pressure (Soubra et al. 2003b). Therefore, there is an urgent need to properly evaluate these reduction coefficients based on rigorous experimental model tests and to perform some theoretical models in agreement with the experimental findings.

This paper is devoted to the determination of the ultimate bearing capacity of a strip footing resting on a horizontal ground surface and subjected to a complex loading based on a centrifuge experimental model and a theoretical limit analysis model. It should be emphasized that complex loading is a frequent load for an offshore structure founded on the sea-bed. It results from both vertical loading (weight of superstructures, overloading, etc.) and horizontal loading (e.g. wave, wind, earthquake).

First, a brief description of the experimental small scale model is given. Then, a presentation of some useful experimental results follows. Some insights into the footing kinematics due to several complex loading are given. Finally, the kinematically admissible failure mechanisms used for the computation of the ultimate bearing capacity under several loading configurations are presented. The paper concludes by a comparison between the experimental findings of the ultimate bearing pressures and the theoretical solutions given by the limit analysis theory for different complex load configurations.

It should be mentioned that similar comparisons between centrifuge experimental results and upper-bound solutions from limit analysis theory have been made by Soubra et al. (2003a) in the case of an eccentric loading and Soubra et al. (2003b) in the case of an inclined loading. Also, the effect of the proximity of a slope on the bearing capacity of a strip footing was investigated by Soubra et al. (2004) in the case of a vertical load and Thorel et al. (2004) in the case of a complex loading.

2 CENTRIFUGE MODELLING

Physical modelling with centrifuge, a widespread technique in the geotechnical field (Corté 1988, Ko et al. 1991, Leung et al. 1994, Kimura et al. 1998 & Phillips et al. 2002), makes it possible to reproduce *in situ* stresses in a small scale model. The full-scale geotechnical model, named prototype (P) and the small scale model (M) are linked together through scaling laws, deduced from equilibrium equations. The main scaling factors $x^* = X^M/X^P$ used in this study are listed on Table 1 in which N is the centrifuge acceleration or 'g-level'.

2.1 *Experimental program*

Data presented here have been extracted from several experiments performed in the LCPC on shallow foundations (Bakir 1993, Bakir et al. 1994, Maréchal et al. 1998, Maréchal 1999, Garnier et al. 2000 and Assaf 2004). The tests concern the cases of inclined and/or eccentric load, and the foundation may be placed in the proximity of a slope, at a distance d from the crest of the slope. Figure 1 shows the different geometrical parameters used in the analysis. In this paper, only tests on a horizontal ground surface ($\beta = 0$) and those where the footing edge is placed at a distance d greater than 6B from the crest of the slope have been presented. No embedment of the foundation (i.e. $D = 0$) is considered here. Several sets of parameters have been tested : e/B = 0, 1/8; $\delta = 0$, 15°, −15° and 20°.

Table 1. Scaling factors.

Parameter	Scaling factor
Length, Displacement	$\ell^* = 1/N$
Density	$\rho^* = 1$
Acceleration	$g^* = N$
Stress	$\sigma^* = 1$
Force	$F^* = 1/N^2$
Angle of rotation	$\alpha^* = 1$

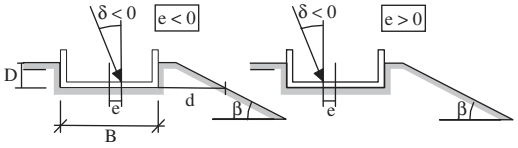

Figure 1. Notations used in complex loading of footings.

2.2 *Experimental setup*

A rectangular strong box (120 cm × 80 cm) as shown in Figure 2 has been filled with white Fontainebleau sand using dry raining technique (Garnier et al. 1999). The main characteristics of the white Fontainebleau sand are presented in Tables 2 and 3. Following the results from Ovesen (1979), the scale effect can be neglected if $B^M/D_{50} > 30$. Here, as $B^M = 40$ mm, the ratio B^M/D_{50} is about 180.

A typical strong box includes 6 foundations of width B = 40 mm and length L = 280 mm. It is divided into 2 lanes delimited by 3 vertical thick glass plates (Figs 2–4), which were used in order to simulate plane strain conditions. When the strong box is filled up, the surface of the sand mass is levelled.

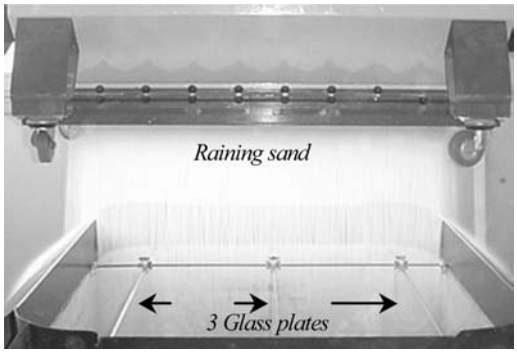

Figure 2. Raining of dry sand using an automatic mobile hopper.

Table 2. Fontainebleau sand characteristics.

ρs (kg/m^3)	(ρ_d)min (kg/m^3)	$(\rho d)_{max}$ (kg/m^3)	c′ (kPa)	φ′ (degrees)
2650	1422	1739	0–6*	39–40°*

*$\gamma_d = 16$ kN/m^3 and normal stress ranging from 50 to 300 kPa.

Table 3. Particle size analysis of Fontainebleau sand.

Particle size (mm)	0.80	0.50	0.315	0.2	0.125	0.08	0.05
Finer (%)	100	99.9	96.1	31.7	4.1	2.6	2.3

Four calibrated boxes (Fig. 4), laying on the floor of the strong box are used to check the density of the sand model. As a rain gauge gives a sample of the mass of water rained, the density of sand is obtained from the average mass of sand rained in those boxes during pluviation. At the end of a centrifuge test, the strong box is emptied and calibrated boxes are levelled and weighed.

2.3 *Devices and loading process*

The geotechnical centrifuge at LCPC laboratory, Nantes (Corté & Garnier 1986) has a radius (distance axis/ basket platform) of 5.50 m.

Two different accelerations have been used during the tests (Fig. 5) : the 50 g … ("M" type foundations with $B^P = 2$ m and $B^M = 40$ mm) and the 30g ("B" type foundations with $B^P = 0.9$ m and $K^M = 30$ mm). Also, two types of model foundations have been used to simulate two different widths (2 m and 0.9 m) of the prototypes.

The foundations are made of aluminium. Sand particles are glued at the footing base to simulate rough base conditions. However, the footing sides are kept smooth. Finally, friction at the glass-footing interface (Figs. 3–4) has been reduced with Teflon strips fixed on the footing. Both foundations are 4 mm thick and 280 mm long (i.e. L/B = 7 for "M" footing type and L/B = 9.33 for "B" footing type).

The upper faces of the footings are equipped with semi-cylindrical joints (Fig. 5) which can be placed on the footing centreline or eccentrically (e/B = 1/8). This allows the foundation to rotate freely around the load application point.

The loading device consists of a hydraulic servo controlled jack with a force transmission rod equipped with a ball joint in its middle part (Fig. 6). This system allows the foundation to move freely in the horizontal direction without any spurious moment in the transmission rod.

The load applied to the model is measured using a 5000 daN transducer placed on top of the jack and linked to the transmission rod. The displacement of the rod is also measured during loading (Fig. 6). The displacement of the foundation is measured using four LVDT transducers placed on its corners (Fig. 7). Three of these transducers measure the vertical displacements, and the last one gives the horizontal displacement.

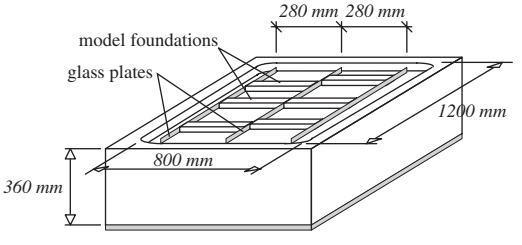

Figure 3. Scheme of a strongbox equipped with glass plates.

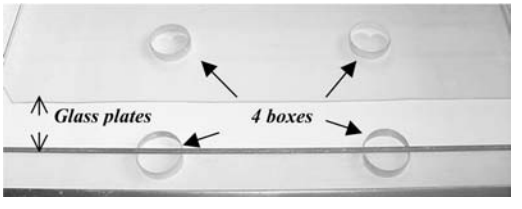

Figure 4. Layout of the density boxes: 2 boxes per lane.

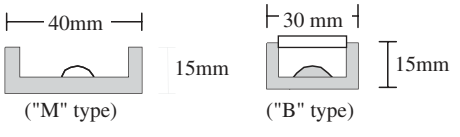

Figure 5. Model foundations used in the tests.

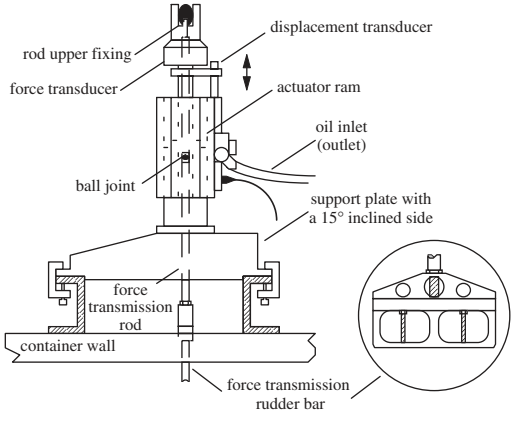

Figure 6. Side view of the loading device and detail of the force transmission rudder bar.

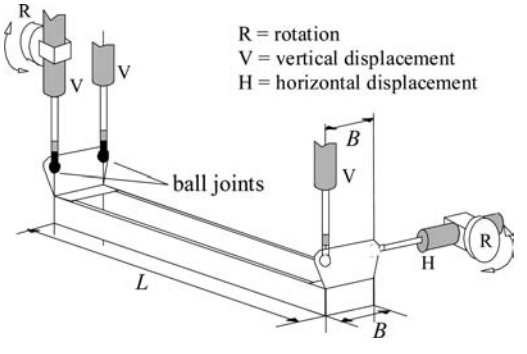

Figure 7. Location of the displacements transducers on the foundation.

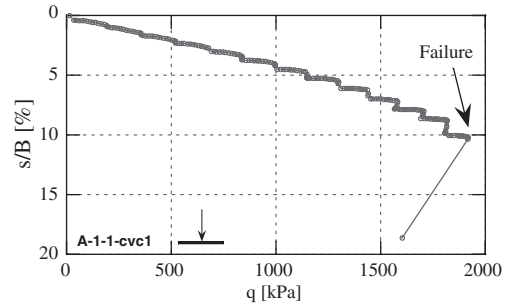

Figure 8. Example of loading curve (test A-1-1 : vertical central load).

Two other transducers measure the rotation of the footing.

Each strong box follows the same experimental setup, as described below:

– Preparation of the soil sample and installation in the centrifuge with the foundations, the transducers and the loading device.
– Macrogravity self-weight loading of the soil sample during five 1 g – 50 g cycles.
– Step by step loading of the foundation until failure (Fig. 8).
– Control of the sample density during the emptying of the strong box (embedded calibrated boxes).

The displacement of the centre of the foundation is then calculated by combining these measurements.

3 RESULTS

3.1 *Footing kinematics*

The application of a complex load on a footing may induce different types of movement depending on the direction and intensity of the load. When both e and δ have the same sign (Fig. 1), the moments reported to the footing centre due respectively to horizontal and vertical components have the same sign (i.e. cumulative effect). However, opposite signs of e and δ leads to an antagonistic effect of the moments due to the horizontal and vertical forces.

During each test, the movement of the foundation may be calculated assuming that it is a rigid body with a 2D movement. The displacement of the foundation is determined with one rotation and two displacements (Fig. 9). The kinematics of the strip footing is useful in order to validate the movement predicted by the failure mechanisms used in the limit analysis approach.

Measurements of displacements and rotations make it possible to follow the movement of the base of the foundation (Figs 10–12). This data confirms the

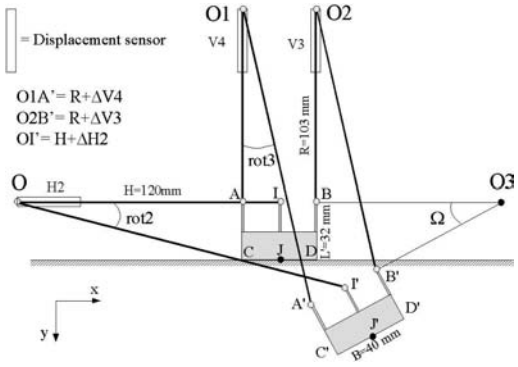

Figure 9. Strip footing in the initial and current position.

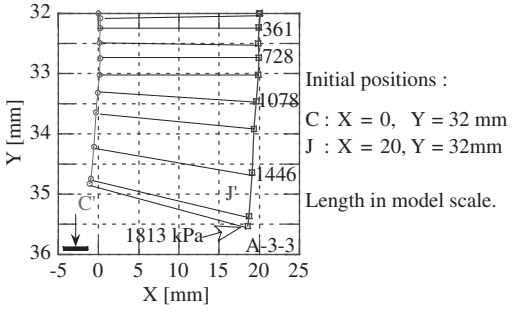

Figure 10. Movement of the foundation base for vertical central loading (e = 0, δ = 0).

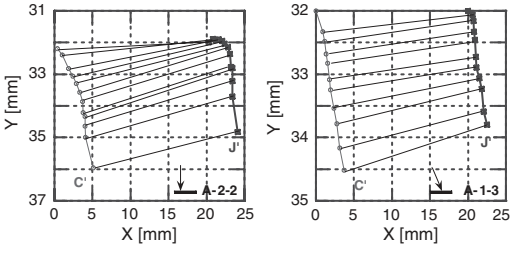

Figure 11. Movement of the foundation base for vertical eccentric loading (left) and inclined central loading (right).

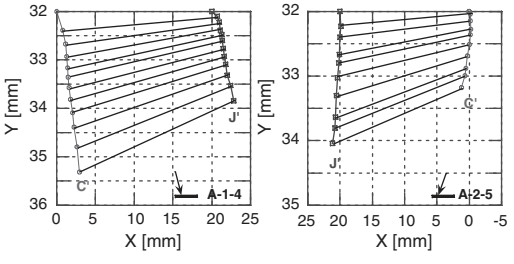

Figure 12. Movement of the foundation base for antagonist loading (left) and cumulative combined loading (right).

Table 4. Experimental and limit analysis results.

Test	γ_d	e/B	δ	(q_r)		$(q_r)_m$		$(q_r)_m/(q_r)_m(0)$	
Test	(kN/m^3)	(−)	(°)	EXP (kPa)	LA (kPa)	EXP (kPa)	LA (kPa)	EXP (−)	LA (−)
A-1-1	16.20	0	0	1916	2140				
A-2-1	16.28	0	0	1673	2148				
A-3-3	16.29	0	0	1813	2150	1808	2138	1	1
M-1-1	16.04	0	0	1734	2125				
M-1-4	16.04	0	0	1908	2125				
M-10-1	16.02	0	0	*825	1156				
M-10-3	16.02	0	0	*888	1156	856	1156		
A-1-3	16.20	0	−15	871	752				
A-3-6	16.29	0	−15	707	755				
M-2-3	15.98	0	−15	844	745				
M-3-4	16.09	0	−15	856	749	800	749	0.44	0.35
M-7-5	16.07	0	−15	848	748				
M-11-2	16.07	0	−15	730	748				
M-11-3	16.07	0	−15	742	748				
M-4-2	16.04	0	−20	569	490				
M-4-6	16.04	0	−20	571	490	553	490	0.31	0.23
M-5-2	16.09	0	−20	519	491				
A-1-2	16.20	1/8	0	1455	1570				
A-2-2	16.28	1/8	0	1439	1576				
M-2-4	15.98	1/8	0	1473	1553	1436	1562	0.79	0.73
M-2-7	15.98	1/8	0	1455	1553				
M-3-2	16.09	1/8	0	1460	1561				
M-4-4	16.04	1/8	0	1333	1557				
A-1-4	16.20	1/8	−15	884	1057				
A-1-5	16.20	1/8	−15	764	1057	802	1058	0.44	0.49
A-2-6	16.28	1/8	−15	759	1061				
A-1-6	16.20	1/8	15	791	592				
A-2-5	16.28	-1/8	−15	643	594	717	593	0.40	0.28
A-2-3	16.28	1/8	20	482	393				
A-2-4	16.28	1/8	20	512	393	497	393	0.27	0.18

*tests performed with a “B type” foundation.
$q_{rm}(0)$ is the mean value for vertical central load (e = δ = 0).

assumptions made of using a non-symmetrical mechanism even for a footing subjected to a vertical load at the centre.

3.2 *Ultimate bearing pressures*

For each loading configuration (i.e. e and δ), Table 4 gives the mean value $(q_r)_m$ of the bearing pressure as given by the experimental (EXP) and theoretical (LA) models. Also, the final two columns of the same table give the reduction coefficients $(q_r)_m/(q_r)_m(0)$ corresponding to different loading configurations using the mean values of the experimental and theoretical results.

The theoretical results are obtained by the kinematical approach of the limit analysis (LA) theory. These values are presented in column “q_r LA” of Table 4. For vertical or inclined central load, the translational multiblock non-symmetrical mechanism presented by Soubra (1999) and Soubra et al. (2003b) is used (Fig. 13). However, when the eccentricity is present, two different rotational failure mechanisms

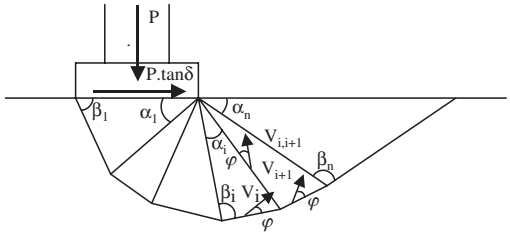

Figure 13. Translational multiblock failure mechanism (Soubra 1999).

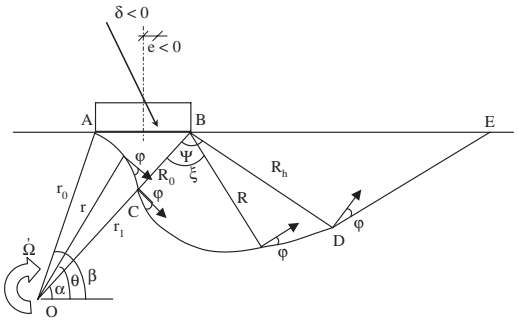

Figure 14. Double-spirals rotational failure mechanism (cumulative loading, Soubra et al. 2003a).

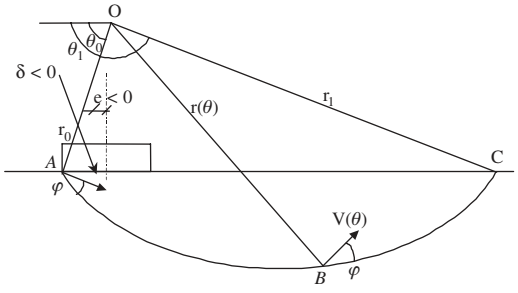

Figure 15. Log-spiral rotational failure mechanism (antagonistic loading, Soubra et al. 2003a).

are employed. When the complex loading leads to a cumulative effect of the load components (cf. δ 3.1), the soil failure is simulated by a double spiral failure mechanism with three different shear zones (Fig. 14). An antagonistic effect of load components is simulated by a rigid block failure mechanism bounded by a log-spiral slip surface (Fig. 15). For both rotational mechanisms, the moments due to horizontal and vertical components of the footing load have the same sign when reported to the rotation centre of the failure mechanism. The laboratory shear strength parameters used in the theoretical models are $c' = 4.5$ kPa, $\varphi' = 39.4°$. These values were obtained by direct shear box tests.

The comparison between centrifuge results and theoretical solutions given by the kinematical approach of limit analysis for the different load combinations is presented in Figure 16 and Table 4. Reasonably good agreement between experimental and theoretical results is observed in terms of both the ultimate bearing pressures and the reduction coefficients. It can be seen that the experimental results do not differ from the LA predictions by more than 34% (with a mean value of 15%) for a given loading configuration. The discrepancy may be attributed mainly to the ageing effect of the re-used sand (Thorel et al. 2003) and the

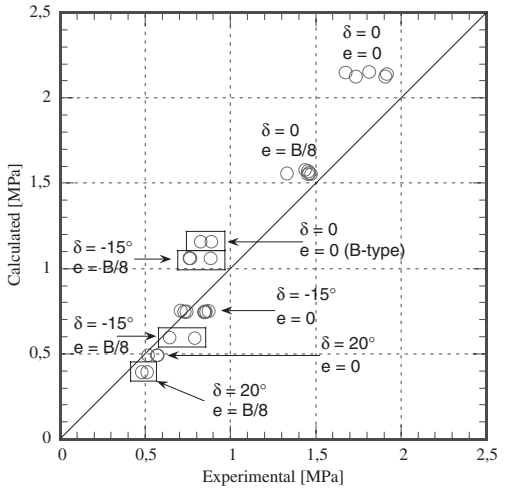

Figure 16. Calculated failure stress versus experimental one.

loading process of the footing, particularly for inclined loading.

It should be emphasized that the comparison between the experimental and the theoretical results have shown that the LA results are, as expected, greater than the experimental results for all loading configurations except those that include loading inclination. This remark may indicate that the present theoretical models do not properly simulate the experimental model which may include a velocity discontinuity along the soil-footing interface. This discontinuity will induce an energy dissipation along this interface and increases the bearing capacity of the footing. Further work should be undertaken to study the possible effect of this discontinuity on the bearing capacity of the foundation.

4 CONCLUSIONS

Strip footings resting on a horizontal sandy soil subjected to inclined and/or eccentric loading have been investigated from an experimental and a theoretical point of view using respectively centrifuge modelling and limit analysis theory. Reasonably good agreement is obtained between experimental and theoretical results in terms of the ultimate bearing capacity and the reduction coefficients for several load combinations. The experimental findings have shown that even for vertically loaded footings without any load eccentricity, the failure mechanism is non-symmetrical if the foundation is free to rotate. Further work should investigate more elaborate mechanisms that may include a velocity discontinuity along the soil-footing interface when the footing load is inclined. Additional

tests may be undertaken in the future to study the case of a and frictional cohesive soil material.

ACKNOWLEDGEMENTS

The authors would like to thank C. Favraud and N. Thétiot for their help to perform centrifuge tests.

REFERENCES

Assaf R. 2004 Fondations superficielles établies sur sol horizontal et soumises à des chargements inclinés et excentrés. Etude expérimentale sur modèle réduit centrifugé de la capacité portante et du mouvement de la fondation. *Rapport LCPC* RMS/MSC n°2004-4-04-1/1-a. 249.

Bakir N.-E. 1993. Etude sur modèles centrifugés de la capacité portante de fondations superficielles. *Thèse Ecole Centrale de Nantes*. Juin. 276.

Bakir N-E., Garnier J., Canepa Y. 1994. Etude sur modèles centrifuges de la capacité portante de fondations superficielles. *Etudes et recherches des LPC*. GT 59. Octobre. 188.

Caquot A. & Kérisel J. 1953. Sur le terme de surface dans le calcul des fondations en milieu pulvérulent. *Proc. 3rd Int. Conf. on Soil Mech. And Found. Engrg., ICOSOMES, Zurich*, Vol. I, 336–337.

Corté J.F. (ed) 1988. *Centrifuge 88*. Proc. Int. Conf. on geotechnical centrifuge model. Paris. 25–27 Paris. 610.

Corté J.F. & Garnier J. 1986. Une centrifugeuse pour la recherche en géotechnique. *Bulletin de liaison des laboratoires des Ponts et Chaussées*. 146. 5–28.

DTU 13.12. 1988. Règles pour le calcul des fondations superficielles. *Cahier CSTB*, Paris, AFNOR DTU P11-711, 28–30.

Eurocode 7. 1996. Calcul géotechnique. XP ENV 1997-1.

Fascicule 62 Titre V. 1993 Technical rules of design and calculation of the foundations of the works of Civil Engineering. *M.E.L.T.* – Ministère de l'équipement, du Logement et des Transports. 182.

Garnier J., Amar S., Mezazigh S., Maréchal O. 2000. New results for slope-foundation interactions. *GEOENG 2000. Melbourne.*

Garnier J., Derkx F., Cottineau L.-M., Rault G. 1999. Etudes géotechniques sur modèles centrifugés. Evolution des matériels et des techniques expérimentales. *Bulletin de liaison des laboratoires des Ponts et Chaussées*. 223. 27–50.

Kimura T., Kusakabe O, Takemura J. (ed) 1998. *Int. Conf. Centrifuge 98*. Tokyo, Balkema. 919.

Ko H.Y. & McLean F. (ed). 1991. *Int. Conf. Centrifuge 91*. Boulder. 13–14 June. Balkema. 616.

Leung C.F., Lee F.H., Tan E.T.S. (ed). 1994. *Int. Conf. Centrifuge 94. Singapore*. 31 aug–2sep. Balkema. 836.

Maréchal O., Garnier J., Canepa Y., Morbois A. 1998. Bearing capacity of shallow foundations near slopes under complex loads. *Centrifuge 98. Tokyo.* vol.1. 459–464.

Maréchal. O. 1999. Portance de fondations superficielles établies à proximité de talus et soumises à des charges inclinées et excentrées. *Thèse Doct. Univ. de Nantes*. 357.

Ovesen N.K. 1979. The scaling law relationships. Design parameters in geotechnical engineering, *7th E.C.S.M.F.E., Brighton,* Vol. 4, 319–323.

Phillips R., Guo P.J., Popescu R. 2002. *Physical modelling in Geotechnics. ICPMG 02*. Balkema. 1025.

Soubra A.H., Garnier G., Thorel L. 2003a. Effet de l'excentre-ment de la charge sur la portance des fondations superficielles: Etude théorique et expérimentale. *Symp. Int. FONDSUP 5–7 nov., Paris* Magnan & Droniuc (ed.) 455–462.

Soubra A.H., Thorel L., Garnier J. 2003b. Effet de l'inclinaison de la charge sur la portance des fondations superficielles: Etude théorique et expérimentale. *Symp. Int. FONDSUP 5–7 nov., Paris* Magnan & Droniuc (ed.) 463–470.

Soubra A.H., Garnier J., Thorel L., Chambon P., El Hachem E., Cortas J., Oueidat H., Chehade R. 2004. Portance des fondations superficielles établies à proximité d'une pente : étude théorique et expérimentale. *Coll. int. Géotechnique. Beyrouth. 19–22 mai*. 6.

Soubra. A.-H. 1999. Upper-bound solutions for bearing capacity of foundations. *J. of Geotech. & Geoenv. Engrg., ASCE*. 125(1). 59–68.

Thorel L., Gaudin C., Rault G., Garnier J. 2003. Vieillissement des sols reconstitués utilisés sur les modèles physiques en centrifugeuse. IS LYON 03. *3rd Int. Symp. On Deformation Characteristics of Geomaterials. Lyon 22–24 sept 03*. Di Benedetto et al. (ed.). Balkema. 89–96.

Thorel L., Soubra A.H., Garnier J., Chambon P., El Hachem E., Cortas J., Oueidat H., Chehade R. 2004. Effet d'un chargement complexe sur la portance des fondations superficielles établies à proximité d'une pente : étude théorique et expérimentale. *Coll. int. Géotechnique Beyrouth. 19–22 mai*. 6.

Vesic A.S. 1975. Bearing capacity of shallow foundations. In : *Foundation engineering handbook,* Winterkorn & Fang (ed.). Van Nostrand, 121–147.

NOTATION

γ_d = unit weight of dry soil
β = angle of the slope with the horizontal
δ = load inclination
φ' = effective angle of internal friction
$(\rho_d)_{max}$ = maximum density of dry soil
$(\rho_d)_{min}$ = minimum density of dry soil
ρ_s = density of solid particles
B = breadth of foundation
c′ = effective cohesion intercept
D = embedment depth
D_{50} = diameter corresponding to 50% finer
e = eccentricity
g = centrifuge acceleration
L = length of foundation
P = vertical component of the applied force
q = applied stress
q_r = failure stress
$(q_r)_m$ = mean failure stress of a loading configuration
s = settlement